AGU ADVANCING EARTH AND SPACE SCIENCE

Geophysical Research Letters

RESEARCH LETTER

10.1029/2022GL099096

The Role of Mid-latitude Westerly Jet in the Impacts of November Ural Blocking on Early-Winter Warmer Arctic-Colder Eurasia Pattern

Xinping Xu[1], Shengping He[2,3,4], Botao Zhou[1], Huijun Wang[1,4,5], and Stephen Outten[3]

[1]Collaborative Innovation Center on Forecast and Evaluation of Meteorological Disasters/Key Laboratory of Meteorological Disaster, Ministry of Education, Nanjing University of Information Science and Technology, Nanjing, China, [2]Geophysical Institute, University of Bergen and Bjerknes Centre for Climate Research, Bergen, Norway, [3]Nansen Environmental and Remote Sensing Center and Bjerknes Centre for Climate Research, Bergen, Norway, [4]Nansen-Zhu International Research Centre, Institute of Atmospheric Physics, Chinese Academy of Sciences, Beijing, China, [5]Southern Marine Science and Engineering Guangdong Laboratory, Zhuhai, China

Key Points:

- Early-winter atmospheric response to November Ural blocking (UB) anomalies is sensitive to the background state of westerly jet
- Strong UB with sufficiently weakened westerly jet in November can induce a warmer Arctic-colder Eurasia pattern in December
- The weakened westerly wind waveguide promotes stronger upward propagation of planetary waves forced by UB anomalies

Supporting Information:

Supporting Information may be found in the online version of this article.

Correspondence to:

S. He,
Shengping.He@uib.no

Citation:

Xu, X., He, S., Zhou, B., Wang, H., & Outten, S. (2022). The role of mid-latitude westerly jet in the impacts of November Ural blocking on early-winter warmer Arctic-colder Eurasia pattern. *Geophysical Research Letters*, *49*, e2022GL099096. https://doi.org/10.1029/2022GL099096

Received 13 APR 2022
Accepted 25 JUL 2022

Abstract

Based on statistical analysis using observations and idealized model simulations, previous studies have revealed the potential response of early-winter atmospheric circulation and temperature anomalies to November Ural blocking (UB) anomalies. Using a large number of coupled simulations, this study found that the response is sensitive to the intensity of November mid-latitude westerly jet over Eurasia. Stronger-than-normal November UB without a significantly weakened westerly jet could not cause significant atmospheric response in early-winter. By contrast, stronger-than-normal November UB with a significantly weakened jet would be followed by a warmer Arctic-colder Eurasia (WACE) pattern in December. The significantly weakened westerly jet favors stronger upward propagation of planetary waves, which causes stronger weakening and longer persistence of the stratospheric polar vortex. This stratospheric response persists into December and propagates downward into the troposphere interfering with planetary waves (especially wavenumber-1). The lead-lag UB-WACE linkage modulated by mid-latitude jet may have implications for sub-seasonal predictability.

Plain Language Summary

Observations and idealized model simulations have shown that strong Ural blocking (UB) anomalies in November can induce the "warmer Arctic, colder Eurasia" anomaly in the following December. In this study, a large number of coupled simulations are employed. The results show that the impact of November UB on early-winter Arctic-Eurasian temperature is sensitive to the intensity of November mid-latitude (around 60°N) westerly jet over Eurasia. When November UB anomalies are accompanied by a significantly weakened mid-latitude westerly jet, early-winter would experience a warmer Arctic-colder Eurasia pattern. The significantly weakened westerly wind waveguide is favorable for stronger upward propagation of planetary waves caused by UB anomalies, which leads to persistent atmospheric response in the following December.

1. Introduction

Ural blocking (UB) is a major internal mode of tropospheric atmospheric flow and a key source of predictability of Eurasian climate (Martius et al., 2009; Peings, 2019). The role of UB in causing cold spells across Eurasia is of great importance (Yao et al., 2017). Linkages between UB and Arctic climate change have been extensively investigated (He et al., 2020; Mori et al., 2014; Tyrlis et al., 2020). Arctic sea ice decline and/or Arctic warming can cause tropospheric atmospheric responses through changing anomalous turbulent heat flux and induce an anomalous anticyclone over Northern Eurasia (e.g., a strengthened UB) that causes cold weather over East Asia (Honda et al., 2009; Liu et al., 2012; Peng et al., 2022). Autumn Arctic sea ice loss may influence the stratospheric polar vortex by enhancing upward propagating planetary waves which subsequently cause tropospheric anticyclonic anomalies over Northern Eurasia (Cohen et al., 2014; Kim et al., 2014; Nakamura et al., 2015). On the other hand, atmospheric circulations associated with UB in winter (i.e., December–February) can amplify the warmer Arctic-colder Eurasia (WACE) pattern and sea ice decrease through accumulating more heat over the Barents-Kara Seas (Blackport et al., 2019; Luo et al., 2016). Gong and Luo (2017) revealed that sea ice decline over the Barents-Kara Seas is a delayed response to UB on the weekly time scale, due to enhanced downward infrared radiation related to moisture flux increase caused by UB anomalies. Numerical simulations of Peings (2019) indicated that UB in November can serve as a driver of the WACE pattern and sea ice anomalies. Tyrlis et al. (2020) further identified the strong role of winter UB on driving the WACE pattern from a daily perspective.

Tropospheric UB has been regarded as a precursor to the weakening of the stratospheric polar vortex (Martius et al., 2009) because it can trigger upward propagation of planetary waves from the troposphere into the stratosphere (Nishii et al., 2011). Accompanied with strengthened UB, significantly weakened westerly wind may emerge at mid- and high-latitude Eurasia (Liu et al., 2012; Xu et al., 2019), which is favorable for the vertical propagation of Rossby waves along the polar wave guide (Dickinson, 1968). Based on a case study of extreme events, Tyrlis et al. (2019) showed that UB development in late autumn 2016 drove vertically propagating of planetary waves that weakens the stratospheric polar vortex, followed by extreme cold surges over Eurasia in early winter. The weakened polar vortex tends to be manifest at the surface as the negative phase of Arctic Oscillation (Kim et al., 2014) and modulates the transport of cold air over Eurasia (Huang et al., 2021). The precursor role of November UB on the stratosphere involving the troposphere-stratosphere dynamic coupling was highlighted by Peings (2019) who imposed UB anomalies in a high-top model by a nudging technique.

As summarized above, UB development has been recently regarded as a key preceding signal of the change in the stratospheric polar vortex (Cohen & Jones, 2011; Peings, 2019) and Arctic climate variability (Gong & Luo, 2017). Particularly, the potential impact of November UB on the early-winter WACE pattern provides valuable mechanism for sub-seasonal climate prediction (Peings, 2019; Tyrlis et al., 2019). However, these studies are based on statistically observational analysis and idealized simulations. It remains unclear whether such a mechanism is well reproduced by more comprehensive coupled simulations, which is important for its implementation to sub-seasonal climate prediction.

In this study, we investigate the precursor role of November UB on early-winter Arctic-Eurasian temperature anomalies by using the output from both the Community Earth System Model Large Ensemble (CESM-LE) and the Sixth phase of the Coupled Model Intercomparison Project (CMIP6). It is further revealed that the impact of November UB on early-winter WACE pattern depends on the intensity of November mid-latitude westerly jet which can modulate the vertical propagation of planetary waves. This conclusion may have implications for enhancing the sub-seasonal predictability of temperature anomalies over the Arctic-Eurasian regions.

2. Data and Methods

The analysis used three sets of coupled simulations. The 40-member ensemble of historical simulations for 1920–2005 and future projections for 2006–2100 from the CESM-LE are examined (Kay et al., 2015). Each ensemble member is subject to the same radiative forcing of greenhouse gases but starts with a small random difference to their initial air temperature fields (order of 10^{-14} K). Historical simulations (r1i1p1f1) for 1850–2014 from 40 fully coupled general circulation models (CGCMs) in CMIP6 (Table S1 in Supporting Information S1) are examined (Eyring et al., 2016). The 50 ensemble members of CanESM2 historical simulations for 1979–2020 are also employed. In addition, monthly atmospheric data for 1979–2021 from the fifth generation European Center for Medium-Range Weather Forecasts reanalysis (ERA5) are employed (Hersbach et al., 2020).

The polar cap height (PCH) is defined as area-averaged geopotential height north of 65°N from 1000 to 10 hPa (Cohen et al., 2018). The stratospheric polar vortex index is defined as normalized negative PCH at 50 hPa. The UB index is defined as area-averaged 500 hPa geopotential height in the domain (45°–80°N, 10°W–80°E) (Peings, 2019). The mid- and high-latitude westerly wind index is defined as area-averaged 300 hPa zonal wind in the domain of a parallelogram (from 50°–60°N, 20°E to 60°–70°N, 110°E; red box in Figure S1a in Supporting Information S1) where the maximum deceleration associated with November UB anomalies is located (Figure S1 in Supporting Information S1). For CESM-LE output, the strong/weak UB is identified when UB index is above/below 0.5/−0.5 standard deviation (STD). The November cases of strong UB with significantly weakened WW (~60% of total strong UB November) are identified when UB index exceeds 0.5 STD and WW index is below −0.5 STD; while the November cases of strong UB without significantly weakened WW (~40% of total strong UB November) are identified when UB index is above 0.5 STD and WW index is above −0.5 STD. The same method is applied to CMIP6 simulations. Before the analysis, we have subtracted the least

10.1029/2022GL099096

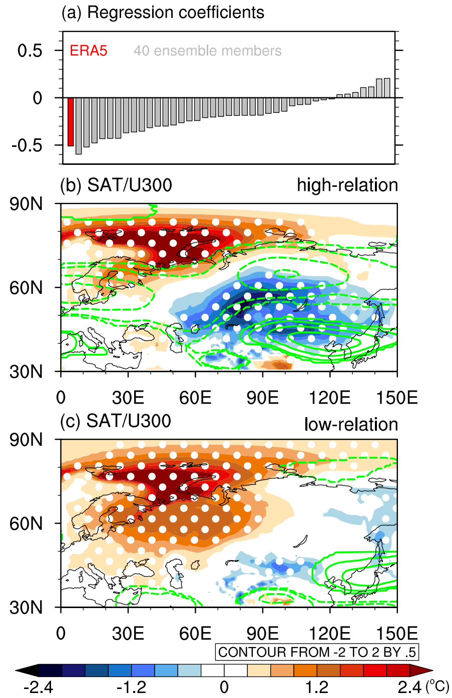

Figure 1. (a) Regression coefficients of December SAT over Eurasia (40°–60°N, 60°–120°E) against the November Ural blocking (UB) index, from ERA5 during 1979–2020, and from 40 ensemble members of CESM-LE during 1920–2099. (b and c) Composite of December SAT anomalies (shading; °C) and 300 hPa zonal wind anomalies (contours; m/s) between the strong and weak UB November during 1920–2099, from (b) 20% high-relation ensembles and (c) 20% low-relation ensembles of CESM-LE. Regions with significant anomalies above the 95% confidence level are marked with dots and all contours exceed the 95% confidence level.

squares quadratic trend from the output of CESM-LE and CMIP6 simulations to remove the underlying global warming trend.

3. Results

We first investigate the potential relationship between November UB activity and climate anomalies in the following December based on CESM-LE output. The regression coefficient of December SAT over central Eurasia onto November UB index is −0.5 in ERA5, but ranges from −0.6 to 0.2 among the 40 ensemble members of the CESM-LE (Figure 1a). Approximately 20% of the ensemble members show a statistically significant relationship, corresponding to the "20% high-relation ensembles" mentioned below. This means that internal variability can affect the lead-lag relationship between November UB activity and the following December climate (Figure 1a). The regression coefficient shows a similar spread in the CMIP6 models (Figure S2 in Supporting Information S1). To understand such an effect of internal variability, we have selected 20% of the ensemble members that show the most negative regression coefficients (i.e., the eight ensembles indicated by the first eight gray bars in Figure 1a) (hereafter referred to as the 20% high-relation ensembles); meanwhile, we have selected another 20% of the ensemble members (hereafter referred to as the 20% low-relation ensembles) that show the least negative regression coefficients (i.e., the eight ensembles indicated by the last eight bars in Figure 1a). These two groups of ensemble members are selected for composite analysis. As expected, the 20% high-relation ensembles have shown clearly that intensified UB in November is generally followed by a significant WACE pattern in December which displays significant cold anomalies over central Eurasia and a warming center over the Barents-Kara Seas (Figure 1b; shading). Accompanying the anomalous WACE pattern, WW decelerates significantly across mid- and high-latitude Eurasia from 50°N to 70°N (Figure 1b; contours). Comparatively, the 20% low-relation ensembles exhibit extensive warmer temperatures from Barents-Kara Seas to Ural regions; but the significant colder anomalies are weaker and greatly reduced in area, with greatly reduced significant WW anomalies across northern Eurasia (Figure 1c). The differences between ensemble members in simulating the lead-lag UB-WACE linkage mean that the early-winter atmospheric response to November UB activity is sensitive, and is suggestive of the potential role played by internal atmospheric variability.

Previous studies have suggested that persistent UB anomalies can increase upward propagation of planetary waves that weakens the stratospheric polar vortex (Martius et al., 2009; Peings, 2019). The stratospheric polar vortex tends to be weakened (strengthened) in December when preceded by a November with strong (weak) UB activities (Figure S3 in Supporting Information S1). It has also been shown that the deceleration of tropospheric westerly flow is favorable for upward wave propagation (Charney & Drazin, 1961). Considering the wave-mean flow interaction theory proposed by Charney and Drazin (1961), we therefore hypothesize that the previously revealed UB-related stratospheric pathway for the delayed surface impact might be different when the WW significantly decelerates.

To test this hypothesis, we illustrate the December atmospheric anomalies in two different categories using both CESM-LE and CMIP6 output. One contains the Decembers that follow Novembers experiencing strong UB with significantly weakened WW, while the other contains the Decembers that follow Novembers experiencing strong UB without significantly weakened WW. Following strong UB with significantly weakened WW in November, an anomalous WACE pattern coinciding with decelerated jet stream in December has been simulated by both CESM-LE and CMIP6 ensembles (Figures 2a and 2c). This climate anomaly pattern bears great resemblance to that in Figure 1b. In contrast, no significant Eurasian cold anomalies emerge in December when November WW is not dramatically decelerated with UB still significantly stronger than normal (Figures 2b and 2d). December following strong UB without weakened WW in November also lacks a warming center over the Arctic in CMIP6

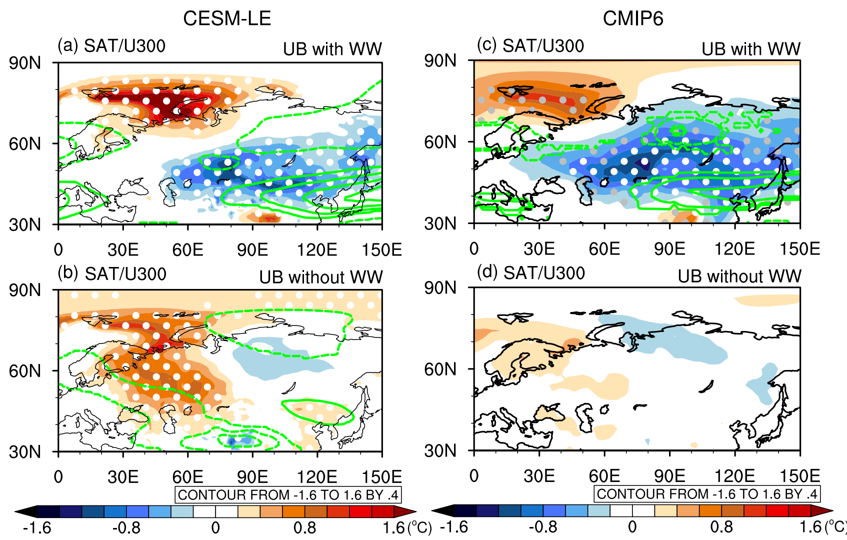

Figure 2. Composites of December SAT anomalies (shading; °C) and 300 hPa zonal wind anomalies (contours; m/s) following (a) strong Ural blocking (UB) with weakened westerly wind (WW) in November and (b) strong UB without weakened WW in November, derived from the 40 ensemble members of CESM-LE during 1920–2099. (c and d) Same as (a and b), but derived from the ensemble mean of 40 CGCMs in CMIP6 historical simulations during 1850–2013. (a and b) Regions with significant anomalies above the 95% confidence level are marked with dots and all contours exceed the 95% confidence level. (c and d) Temperature/zonal wind anomalies where more than 80% (90%) of the models agree on the sign of the ensemble mean are shown as gray (white) stippling/green contours.

(Figure 2d). Results of Figure 2 imply that the connection of December WACE pattern with preceding November UB activity is sensitive to the condition of decelerated westerlies in November. It should be noted that these results are not sensitive to the threshold of the UB index (Figure S4 in Supporting Information S1). A detailed discussion about how the pathway connecting November UB and early-winter WACE pattern is modulated by mid-latitude westerly jet will be elucidated next.

Figures 3a and 3c illustrate the evolutions of PCH anomalies following strong UB with weakened WW in November in both simulations. Results from CESM-LE show that significant positive PCH anomalies spread across the troposphere and stratosphere, in response to strong UB with significantly weakened WW in November (Figure 3a). This is indicative of a dramatic weakening of the stratospheric polar vortex related to planetary wave activities caused by blocking activity and favored by weakened westerly jet. The PCH response can last throughout November and December for the mid- to upper-troposphere and stratosphere (Figure 3a). Results from CMIP6 exhibit positive PCH anomalies persisting from November to December throughout the stratosphere and troposphere, which is consistent across more than 80% models (Figure 3c). The weaker westerly jet could cause more persistent atmospheric patterns (Francis & Vavrus, 2012). The consistency between CESM-LE and CMIP6 provides strong support for the speculation that significantly weakened November westerly jet stream can promote the persistent influence of November UB on the early-winter stratosphere-troposphere coupling and polar vortex weakening.

However, it is not the case of PCH evolutions following strong UB without weakened WW in November. According to Figure 3b, when November mid-latitude WW is not significantly weakened, the anomalous PCH is much weaker and confined to the stratosphere and upper-troposphere and cannot reach the mid- to lower-troposphere. This finding supports the role of UB anomalies in weakening of the stratospheric polar vortex under the critical condition of the WW being sufficiently weakened. Early theories have suggested that the stationary planetary waves would be evanescent in regions of strong WW and the vertical propagation of planetary waves would be trapped in the troposphere by winter westerly jet (Charney & Drazin, 1961; Dickinson, 1968). In other words, the waveguide is more likely to be formed in regions of sufficiently weakened westerlies (Charney & Drazin, 1961). Then, the physical mechanism in this paper can be understood as follows: the significantly weakened WW waveguide promotes strong upward propagation of planetary wave excited by UB anomalies and favors the persistent impacts of November UB. This is also true when we examine the results based on CMIP6 (Figure 3d). A similar

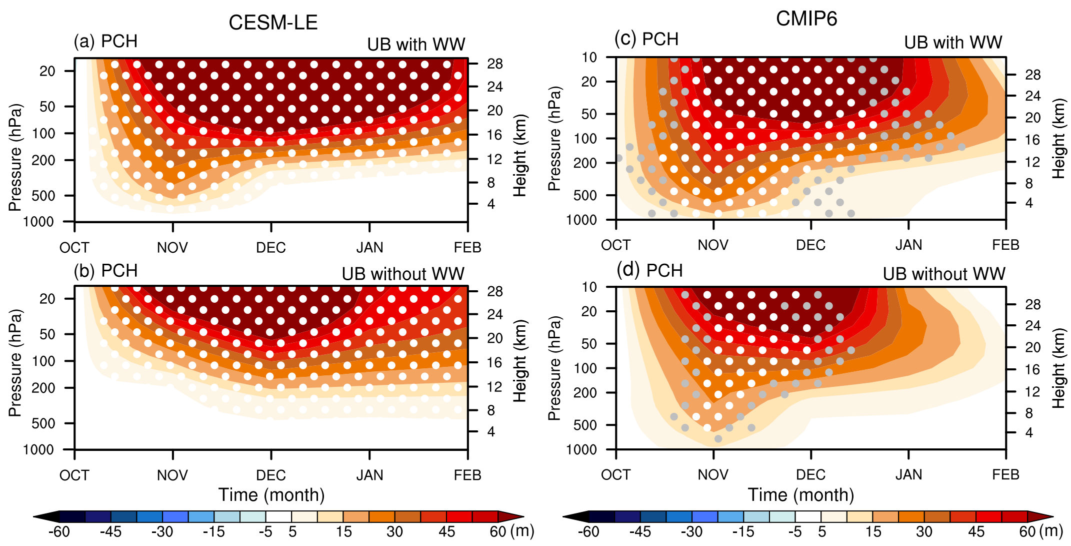

Figure 3. Composites of monthly polar cap height (PCH) anomalies (m) from October to the following February following (a) strong Ural blocking (UB) with weakened westerly wind (WW) in November and (b) strong UB without weakened WW in November, derived from 40 ensemble members of CESM-LE during 1920–2020. Regions with significant anomalies above the 95% confidence level are marked with dots. (c and d) Same as (a and b), but derived from the ensemble mean of 40 CGCMs in CMIP6 historical simulations during 1850–2014. PCH anomalies where more than 80% (90%) of the models agree on the sign of the ensemble mean are shown as gray (white) stippling.

PCH response with much lower magnitude and statistical significance is simulated in a November that experiences strong UB without weakened WW, which rapidly disappears below 200 hPa in December (Figure 3d). Previous studies have revealed that mid-latitude weak westerlies might occur with strong UB anomalies (Liu et al., 2012; Mori et al., 2014) (Figure S1 in Supporting Information S1). It is worth noting that, the westerly flow, which is closely related to the meridional temperature gradient between the lower and higher latitudes, can be influenced by various factors (e.g., anomalous diabatic heating due to variations in sea ice, sea surface temperature and snow cover) (He et al., 2020; Li et al., 2015) in addition to natural variability modes (e.g., blocking events) (Cohen et al., 2014).

Figure 4 shows a clearer picture on the detection of early-winter troposphere-stratosphere dynamic response to November UB anomalies under the modulation of westerly jet. The wave activity in December following strong UB with weakened WW in November, when decomposed into wavenumbers, primarily projects onto the zonal wavenumber-1 pattern. To be specific, the wavenumber-1 component of 300 hPa geopotential height anomalies in December exhibits a significant dipole pattern that is in phase with the long-term climatology (Figures 4a and 4e). Vertically, the significant dipole anomaly can extend from the upper-stratosphere to near-surface (Figures 4c and 4g). Such a constructive interference in planetary waves coincides with the strong dynamic coupling between the stratosphere and troposphere (Kim et al., 2014). The downward coupling that reaches the surface (Figures 4c and 4g) further promotes UB development (Figures S5a, S5c, S5e, and S5g in Supporting Information S1) and thereby leads to warmer temperatures to the north and colder temperatures to the south (Tyrlis et al., 2019; Xu et al., 2018). In contrast, following Novembers experiencing strong UB without weakened WW, the December atmospheric large-scale atmospheric circulation has not exhibited significantly anomalous wavenumber-1 pattern (Figures 4b, 4d, 4f, 4h, and Figures S5b, S5d, S5f and S5h in Supporting Information S1). These findings based on fully coupled climate models, which can also be found in the short reanalysis record (Figure S6 in Supporting Information S1), have indicated the crucial role of westerly jet stream in modulating the lead-lag UB-WACE linkage. This hypothesis also provides some insights into predicting Arctic-Eurasian SAT anomalies in early winter, especially providing insights on how to take into account the effects of internal atmospheric variability.

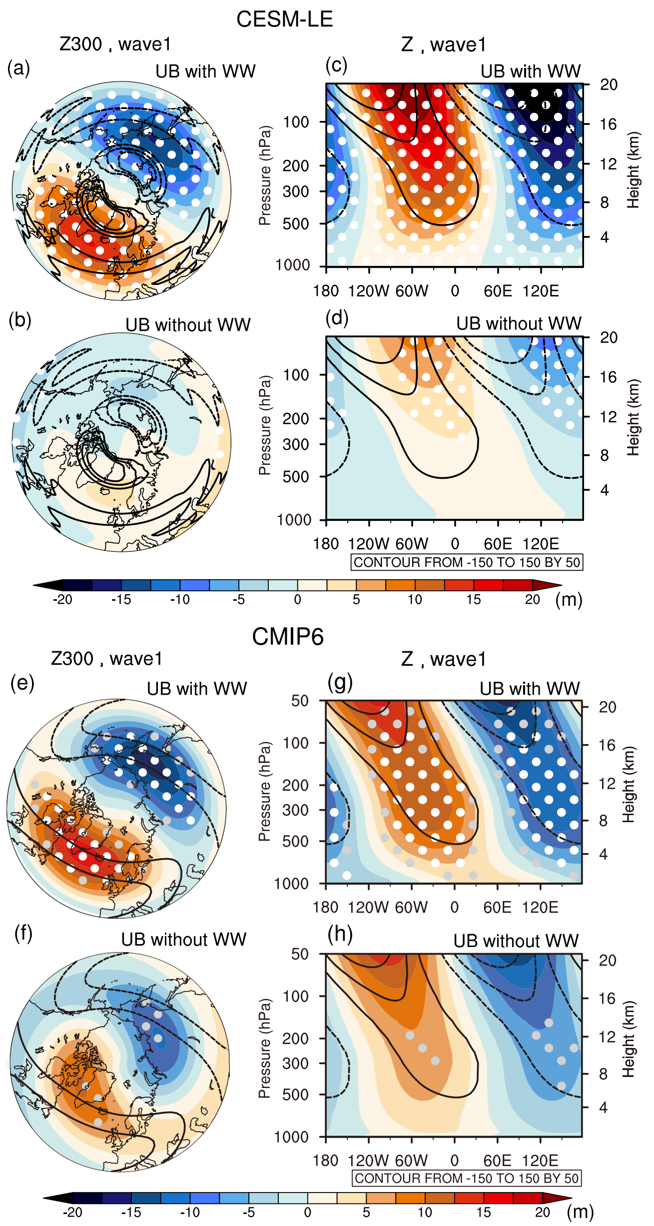

Figure 4. Composites of December (a–b) zonal wavenumber-1 component of 300 hPa geopotential height anomalies (shading; m) following (a) strong Ural blocking (UB) with weakened westerly wind (WW) in November and (b) strong UB without weakened WW in November, derived from 40 ensemble members of CESM-LE during 1920–2099. The composite differences (shading) are compared with the long-term climatology (contours). (c and d) Same as (a and b), but for the longitude-pressure section averaged over 45°N–75°N. Regions with significant anomalies above the 95% confidence level are marked with dots. (e–h) Same as (a–d), but derived from the ensemble mean of 40 CGCMs in CMIP6 historical simulations during 1850–2013. Anomalies where more than 80% (90%) of the models agree on the sign of the ensemble mean are shown as gray (white) stippling.

4. Conclusions

Based on the analysis of both the 40-member ensemble of CESM-LE simulations for 1920–2100 and the 40 CGCMs of CMIP6 historical simulations for 1850–2014, this work reveals that the early-winter atmospheric response to November UB anomalies depends on the intensity of mid-latitude WW. The novel result is that we highlight the modulation of westerly jet stream on the stratosphere-troposphere dynamic response to UB anomalies in coupled climate models.

Different ensemble members of CESM-LE have shown large spread in simulating the previously revealed relationship between November UB and Eurasian climate anomalies in early winter. Similar range is found in the 50 ensemble simulations of the CanESM2, for the same period (1979–2020) as ERA5 (Figure S7 in Supporting Information S1). Only some of the ensemble members can reproduce the UB-related WACE pattern, indicating the strong effect of atmospheric internal variability. This study revealed that a significant WACE pattern could emerge in December when the November UB is significantly intensified together with dramatically decelerated westerlies across mid- and high-latitude Eurasia from 50°N to 70°N. In contrast, Eurasia does not show significant colder temperatures in December in response to intensified November UB that has no simultaneous weakened mid-latitude westerly. Note that the same conclusions can be drawn from the future projections of CESM-LE (i.e., 2006–2099) (Figure S8 in Supporting Information S1).

Strong UB activity with significantly weakened WW in November can force stronger upward propagation of planetary waves, which leads to stronger weakening and longer persistence of the stratospheric polar vortex. The stratospheric response can persist into December and then propagate in the troposphere. The stratosphere-troposphere coupling in December is determined by the constructive interference between climatological and anomalous planetary wavenumber-1 pattern. The downward-propagating zonal wavenumber-1 pattern may further favor the development of UB. Consequently, colder conditions occur over Eurasia and warmer anomalies occur over the Arctic. It is worth noting that above stratospheric-tropospheric pathway associated with the intensified UB can be established only when November mid-latitude westerly jet is sufficiently weakened, because the weaker WW waveguide is favorable for the upward planetary wave propagation (Dickinson, 1968) and more persistent atmospheric patterns (Francis & Vavrus, 2012).

Previous studies generally focus on the UB-WACE linkage in wintertime (Luo et al., 2016; Tyrlis et al., 2020). From the point of view of sub-seasonal predictability (Wang et al., 2022; Yang & Fan, 2022), this work is strongly suggestive of the lead-lag linkage between November UB anomalies and early-winter WACE pattern under specified atmospheric conditions. This understanding will help to better implement the climate dynamics in sub-seasonal climate prediction by taking into account the internal atmospheric variability.

Data Availability Statement

Data used in this study are available:

1. CESM-LE: https://www.cesm.ucar.edu/experiments/cesm1.1/LE/.
2. CMIP6: https://esgf-node.llnl.gov/search/cmip6/. CMIP6 models used can be found in Table S1 of Supporting Information S1.
3. CanESM2: https://crd-data-donnees-rdc.ec.gc.ca/CCCMA/products/CanSISE/output/CCCma/CanESM2/?C=M;O=A.
4. ERA5: https://cds.climate.copernicus.eu/cdsapp#!/search?type=dataset&text=ERA5.

Acknowledgments

This research was supported by the National Natural Science Foundation of China (Grants No. 42025502, 41875118, and 42075030), the Research Council of Norway project BASIC (Grant No. 325440), the State Scholarship Fund by China Scholarship Council (Grant No. 202109045003), and the CONNECTED project (UTF-2016-long-term/10030) funded by UTFORSK Partnership Program.

References

Blackport, R., Screen, J. A., van der Wiel, K., & Bintanja, R. (2019). Minimal influence of reduced Arctic sea ice on coincident cold winters in mid-latitudes. *Nature Climate Change*, *9*, 697–704. https://doi.org/10.1038/s41558-019-0551-4

Charney, J. G., & Drazin, P. G. (1961). Propagation of planetary-scale disturbances from the lower into the upper atmosphere. *Journal of Geophysical Research*, *66*(1), 83–109. https://doi.org/10.1029/jz066i001p00083

Cohen, J., & Jones, J. (2011). Tropospheric precursors and stratospheric warmings. *Journal of Climate*, *24*, 6562–6572. https://doi.org/10.1175/2011jcli4160.1

Cohen, J., Pfeiffer, K., & Francis, J. A. (2018). Warm Arctic episodes linked with increased frequency of extreme winter weather in the United States. *Nature Communications*, *9*(1), 869. https://doi.org/10.1038/s41467-018-02992-9

Cohen, J., Screen, J. A., Furtado, J. C., Barlow, M., Whittleston, D., Coumou, D., et al. (2014). Recent Arctic amplification and extreme mid-latitude weather. *Nature Geoscience*, *7*(9), 627–637. https://doi.org/10.1038/ngeo2234

Dickinson, R. E. (1968). Planetary Rossby waves propagating vertically through weak westerly wind wave guides. *Journal of the Atmospheric Sciences*, *25*(6), 984–1002. https://doi.org/10.1175/1520-0469(1968)025<0984:prwpvt>2.0.co;2

Eyring, V., Bony, S., Meehl, G. A., Senior, C. A., Stevens, B., Stouffer, R. J., & Taylor, K. E. (2016). Overview of the coupled model Intercomparison project phase 6 (CMIP6) experimental design and organization. *Geoscientific Model Development*, *9*(5), 1937–1958. https://doi.org/10.5194/gmd-9-1937-2016

Francis, J. A., & Vavrus, S. J. (2012). Evidence linking Arctic amplification to extreme weather in mid-latitudes. *Geophysical Research Letters*, *39*(6), L06801. https://doi.org/10.1029/2012gl051000

Gong, T., & Luo, D. (2017). Ural Blocking as an amplifier of the Arctic sea ice decline in winter. *Journal of Climate*, *30*(7), 2639–2654. https://doi.org/10.1175/jcli-d-16-0548.1

He, S., Xu, X., Furevik, T., & Gao, Y. (2020). Eurasian cooling linked to the vertical distribution of Arctic warming. *Geophysical Research Letters*, *47*(10), e2020GL087212. https://doi.org/10.1029/2020gl087212

Hersbach, H., Bell, B., Berrisford, P., Hirahara, S., Horányi, A., Muñoz-Sabater, J., et al. (2020). The ERA5 global reanalysis. *Quarterly Journal of the Royal Meteorological Society*, *146*(730), 1999–2049. https://doi.org/10.1002/qj.3803

Honda, M., Inoue, J., & Yamane, S. (2009). Influence of low Arctic sea-ice minima on anomalously cold Eurasian winters. *Geophysical Research Letters*, *36*(8), L08707. https://doi.org/10.1029/2008gl037079

Huang, J., Hitchcock, P., Maycock, A. C., Mckenna, C. M., & Tian, W. (2021). Northern hemisphere cold air outbreaks are more likely to be severe during weak polar vortex conditions. *Communications Earth & Environment*, *2*(1), 147. https://doi.org/10.1038/s43247-021-00215-6

Kay, J. E., Deser, C., Phillips, A., Mai, A., Hannay, C., Strand, G., et al. (2015). The community Earth System model (CESM) large ensemble project: A community resource for studying climate change in the presence of internal climate variability. *Bulletin of the American Meteorological Society*, *96*(8), 1333–1349. https://doi.org/10.1175/bams-d-13-00255.1

Kim, B. M., Son, S. W., Min, S. K., Jeong, J. H., Kim, S. J., Zhang, X., et al. (2014). Weakening of the stratospheric polar vortex by Arctic sea-ice loss. *Nature Communications*, *5*(1), 4646. https://doi.org/10.1038/ncomms5646

Li, F., Wang, H., & Gao, Y. (2015). Extratropical Ocean warming and winter Arctic sea ice cover since the 1990s. *Journal of Climate*, *28*(14), 5510–5522. https://doi.org/10.1175/jcli-d-14-00629.1

Liu, J., Curry, J. A., Wang, H., Song, M., & Horton, R. M. (2012). Impact of declining Arctic sea ice on winter snowfall. *Proceedings of the National Academy of Sciences*, *109*(11), 4074–4079. https://doi.org/10.1073/pnas.1114910109

Luo, D., Xiao, Y., Yao, Y., Dai, A., Simmonds, I., & Franzke, C. L. E. (2016). Impact of Ural blocking on winter warm Arctic-cold Eurasian anomalies. Part I: Blocking-induced amplification. *Journal of Climate*, *29*(11), 3925–3947. https://doi.org/10.1175/jcli-d-15-0611.1

Martius, O., Polvani, L. M., & Davies, H. C. (2009). Blocking precursors to stratospheric sudden warming event. *Geophysical Research Letters*, *36*(14), L14806. https://doi.org/10.1029/2009gl038776

Mori, M., Watanabe, M., Shiogama, H., Inoue, J., & Kimoto, M. (2014). Robust Arctic sea-ice influence on the frequent Eurasian cold winters in past decades. *Nature Geoscience*, *7*(12), 869–873. https://doi.org/10.1038/ngeo2277

Nakamura, T., Yamazaki, K., Iwamoto, K., Honda, M., Miyoshi, Y., Ogawa, Y., & Ukita, J. (2015). A negative phase shift of the winter AO/NAO due to the recent Arctic sea-ice reduction in late autumn. *Journal of Geophysical Research: Atmospheres*, *120*(8), 3209–3227. https://doi.org/10.1002/2014jd022848

Nishii, K., Nakamura, H., & Orsolini, Y. J. (2011). Geographical dependence observed in blocking high influence on the stratospheric variability through enhancement and suppression of upward planetary-wave propagation. *Journal of Climate*, *24*, 6408–6423. https://doi.org/10.1175/jcli-d-10-05021.1

Peings, Y. (2019). Ural Blocking as a driver of early-winter stratospheric warmings. *Geophysical Research Letters*, *46*(10), 5460–5468. https://doi.org/10.1029/2019gl082097

Peng, J., Sun, S., & Chen, B. (2022). Maintenance and development of the Ural high and its contribution to severe cold wave activities in winter 2020/21. *Atmospheric & Oceanic Science Letters*, *15*(2), 100130. https://doi.org/10.1016/j.aosl.2021.100130

Tyrlis, E., Bader, J., Manzini, E., Ukita, J., Nakamura, H., & Matei, D. (2020). On the role of Ural blocking in driving the warm Arctic–cold Siberia pattern. *Quarterly Journal of the Royal Meteorological Society*, *146*(730), 2138–2153. https://doi.org/10.1002/qj.3784

Tyrlis, E., Manzini, E., Bader, J., Ukita, J., Nakamura, H., & Matei, D. (2019). Ural blocking driving extreme Arctic sea ice loss, cold Eurasia, and stratospheric vortex weakening in autumn and early winter 2016–2017. *Journal of Geophysical Research: Atmospheres*, *124*(21), 11313–11329. https://doi.org/10.1029/2019jd031085

Wang, H., Dai, Y., Yang, S., Li, T., Luo, J., Sun, B., et al. (2022). Predicting climate anomalies: A real challenge. *Atmospheric & Oceanic Science Letters*, *15*(1), 100115. https://doi.org/10.1016/j.aosl.2021.100115

Xu, X., He, S., Gao, Y., Furevik, T., Wang, H., Li, F., & Ogawa, F. (2019). Strengthened linkage between midlatitudes and Arctic in boreal winter. *Climate Dynamics*, *53*(7–8), 3971–3983. https://doi.org/10.1007/s00382-019-04764-7

Xu, X., He, S., Li, F., & Wang, H. (2018). Impact of northern Eurasian snow cover in autumn on the warm Arctic–cold Eurasia pattern during the following January and its linkage to stationary planetary waves. *Climate Dynamics*, *50*(5–6), 1993–2006. https://doi.org/10.1007/s00382-017-3732-8

Yang, H., & Fan, K. (2022). Reversal of monthly East Asian winter air temperature in 2020/21 and its predictability. *Atmospheric & Oceanic Science Letters*, *15*(1), 100142. https://doi.org/10.1016/j.aosl.2021.100142

Yao, Y., Luo, D., Dai, A., & Simmonds, I. (2017). Increased quasi stationarity and persistence of winter Ural blocking and Eurasian extreme cold events in response to Arctic warming. Part I: Insights from observational analyses. *Journal of Climate*, *30*(10), 3549–3568. https://doi.org/10.1175/jcli-d-16-0261.1